CASL-U-2017-1331-000

Microstructural Modeling of Dynamic Intergranular and Transgranular Fracture Modes in Zircaloys

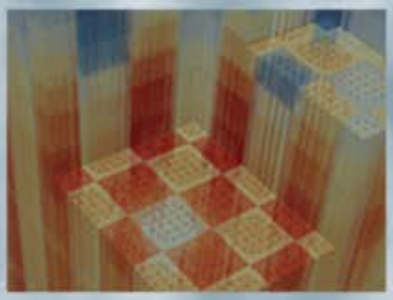

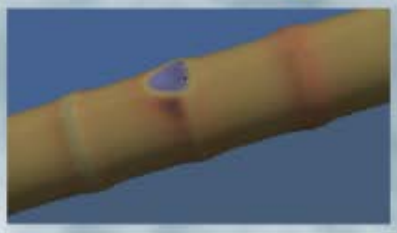

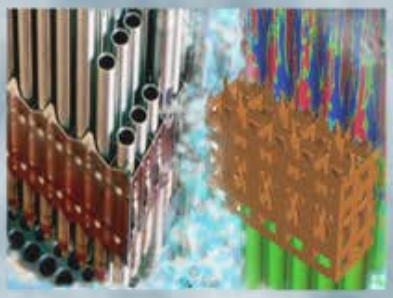

S. Ziaei, North Carolina State University
I. Mohammed,North Carolina State University
M.A. Zikry, North Carolina State University

April 2017

Please complete sections appropriate for this record.

REVISION LOG

Revision	Date	Affected Pages	Revision Description
0	04/30/2017	All	Initial Release

Document pages that are:

Unlimited ___All_____

Export Controlled ___None_____

IP/Proprietary/NDA Controlled__ None _____

Sensitive Controlled___None_____

Requested Distribution:

To:

Copy:

Microstructural Modeling of Dynamic Intergranular and Transgranular Fracture Modes in Zircaloys

Zikry Research Group
North Carolina State University

ABSTRACT

In this time period, we have continued to focus on (i) refining the thermo-mechanical fracture model for zirconium (Zr) alloys subjected to large deformations and high temperatures that accounts for the cracking of ZrH and ZrH2 hydrides, (ii) formulating a framework to account intergranular fracture due to iodine diffusion and pit formation in grain-boundaries (GBs). Our future objectives are focused on extending to a combined population of ZrH and ZrH2 populations and understanding how thermo-mechanical behavior affects hydride reorientation and cracking. We will also refine the intergranular failure mechanisms for grain boundaries with pits.

PERSONNEL

S. Ziaei, Post-Doctoral Associate
I. Mohammed, Ph.D. student
M.A. Zikry, Principal Investigator

SUMMARY OF CURRENT AND FUTURE ACTIVITIES

In support of the work related to CASL's FMC mission, our research group has been focused on developing a high temperature mechanistic fracture model for the cracking of zirconium (Zr) alloys subjected to large deformations and high temperatures. Our group's efforts have been specifically focused on the following objectives:

• Developing a predictive fracture model that tracks failure from nucleation to rupture for mechanistic fracture criteria for zircaloys with hydrides and twins;

• Developing orientation relations (ORS)/interfacial and misfit strain models for f.c.c./Zr-alloys and twins/parent/hydrides. This is a needed step to account accurately for precipitates and hydrides, which have a different crystalline structure than the Zr h.c.p. matrix crystalline structure. This will enable a more detailed understanding of behavior at crystalline interfaces. These OR relations have a pronounced effect on crack nucleation, propagation, and paths;

• We are investigating the effects of twins, in Zr-alloys, on crack nucleation and growth;

• We have been investigating high temperature behavior of pit formation that occurs due to iodine diffusing to the GBs of zircaloys.

DISLOCATION-DENSITY CRYSTALLINE PLASTICITY FORMULATION

We are using a dislocation-density crystalline plasticity formulation to account for aggregate behavior for the h.c.p. crystalline zircaloy matrix, the b.c.c. ZrH and the f.cc. ZrH2 hydrides, and the h.c.p. twin slip-systems. Dislocation-density generation, immobilization, recovery and annihilation can significantly affect overall behavior in h.c.p. materials[1,2]. Experimental studies[3-9] have indicated that self-interactions along the prismatic, basal, and pyramidal planes affect local behavior and deformation mechanisms. We use a dislocation-density based crystalline plasticity formulation that extends previous relevant work by adapting a recently developed dislocation-density crystalline plasticity to investigate immobile and mobile dislocation-density evolution and interactions along the different planes for Zr aggregates. The proposed approach is based on modifying an approach developed by Zikry and Shanthraj [9] that has been used to model dislocation-density interactions and evolution in f.c.c. and b.c.c. polycrystalline aggregates. Based on that framework, we consider all 24 possible dislocation-density self-interactions in h.c.p. crystals by applying Frank's energy criterion to determine the strength of the interactions and the reaction products. These interactions are then to be used with dislocation-density evolution equations that are coupled to a multiple slip crystal plasticity formulation and finite-element techniques for dynamic fracture. These predictions of failure mechanisms in zircaloy-2 and zircaloy-4 along the pyramidal, basal, and prismatic planes will provide fundamental understanding of local fracture behavior that can be used to predict failure paths associated with microstructural fracture with a focus on intergranular and transgranular crack nucleation and propagation.

DISLOCATION-DENSITY CRYSTALLINE PLASTICITY FORMULATION

It can be assumed that, for a given deformed state of the material, the total dislocation-density, $\boldsymbol{\rho^{(\alpha)}}$, can be additively decomposed into a mobile and an immobile dislocation-density, $\boldsymbol{\rho_m^{(\alpha)}}$ and $\boldsymbol{\rho_{im}^{(\alpha)}}$. During an increment of strain on a slip system, a mobile dislocation-density rate is generated and an immobile dislocation-density rate is annihilated. Furthermore, the mobile and immobile dislocation-density rates can be coupled through the formation and destruction of junctions as the stored immobile dislocations act as obstacles for evolving mobile dislocations. These can be combined, see Shanthraj and Zikry [9] for details, into the following equations that relate the immobile and mobile densities to the slip-rates,

$$\frac{d\rho_m^\alpha}{dt} = \left|\dot{\gamma}^\alpha\right|\left(\frac{g_{sour}^\alpha}{b^2}\left(\frac{\rho_{im}^\alpha}{\rho_m^\alpha}\right) - g_{mnter}^\alpha - \rho_m^\alpha - \frac{g_{immob-}^\alpha}{b}\sqrt{\rho_{im}^\alpha}\right), \tag{1}$$

$$\frac{d\rho_{im}^\alpha}{dt} = \left|\dot{\gamma}^\alpha\right|\left(g_{mnter+}^\alpha\rho_m^\alpha + \frac{g_{immob+}^\alpha}{b}\sqrt{\rho_{im}^\alpha} - g_{recov}^\alpha\rho_{im}^\alpha\right), \tag{2}$$

where g_{sour} is the coefficient pertaining to an increase in the mobile dislocation-density due to dislocation sources, $\dot{\rho}_{generation}^{(\alpha)}$, g_{mnter} is the coefficient related to the trapping of mobile dislocations due to forest intersections, cross-slip around obstacles, or dislocation interactions, $\dot{\rho}_{interaction}^{(\alpha)}$, g_{recov} is a coefficient related to the rearrangement and annihilation of immobile

dislocations which is related to $\dot{\rho}^{(\alpha)}_{annihilation}$ and g_{immob} are coefficients related to the immobilization of mobile dislocations which is also shown in $\dot{\rho}^{(\alpha)}_{interaction}$. It should be noted that these coefficients are functions of the immobile and mobile densities, and hence are updated as a function of the deformation mode.

INTERACTION COEFFICIENTS $a_{\alpha\beta}$

The Taylor interaction coefficients, $a_{\alpha\beta}$, are needed to update the reference stress. For the 24 slip-systems for the four slip-planes, these interactions were determined by considering *all* the possible interactions between the 24 slip systems. Sixteen unique interaction types were identified based on Burgers conservation law. These interactions are: self-interactions on the same slip system, co-linear interactions between slip systems with parallel Burgers vectors, co-planar interaction between planar slip systems, and non-planar and non-collinear interactions. There were a total of 576 mobile-mobile interactions and 2088 mobile-immobile interactions for 16 possible interaction types.

COMPUTATIONAL APPROACH

The total deformation rate tensor D_{ij} and the plastic deformation rate tensor D^p_{ij}, are needed to update the material stress state. The method used here is that developed by Zikry [10] for rate-dependent crystalline plasticity formulations, and only a brief outline will be presented here. For quasi-static deformations, an implicit FE method with BFGS iteration is used to obtain the total deformation rate tensor D_{ij}. To overcome numerical instabilities associated with stiffness a hybrid explicit-implicit method is used to obtain the plastic deformation rate tensor D^p_{ij}. This hybrid numerical pattern is also used to update the evolutionary equations for the mobile and immobile densities. The hybrid approach is based on using explicit Runge Kutta, and an implicit Euler method, when numerical stiffness is encountered. Numerical stiffness can be encountered when due to different rate changes along slip systems, slip-rates, resolved shear–stresses, and dislocation-densities can vary widely.

FRACTURE APPROACH

We have adapted a fracture approach that surmounts limitations of current approaches, such as XFEM and cohesive fracture. XFEM is limited by enrichment functions that are based on crack-tip fields that essentially elastic. The limitation of cohesive fracture approaches are that cohesive elements have to, a priori, mapped into regions where fracture is expected. Furthermore, cohesive elements can render the mesh highly compliant, which can lead to numerical instabilities. Hence, we have adapted and modified a method based on overlap elements. In this approach, we consider one element crossed by a crack to be defined implicitly $f(X)=0$, hence dividing the element domain into two subdomains with areas A_{e1} and A_{e2}. Adding phantom nodes on top of the existing nodes, the original cracked element is replaced by two overlapping elements. The two overlapping elements do not share nodes, and therefore can have independent displacement fields. For a 4-node quadrilateral element with one-point integration and hourglass control, the internal nodal force vector of the cracked element is given by

$$f_e^{\text{int}} = f_{e1}^{\text{int}} + f_{e2}^{\text{int}}, \tag{3}$$

where f_{e1}^{int} and f_{e2}^{int} are the internal nodal force vectors of the overlapping elements, and are given by

$$f_{(e1/e2)}^{int} = \frac{A_{(e1/e2)}}{A_0} \int \left[B^T \sigma_{(e1/e2)} \right] dV_e, \tag{4}$$

We have now extended this method to account for crack branching and triple junctions. In summary, the procedure for implementation of the overlapping element method is as follows:

(1) Monitor failure criterion for the necessary elements, at each time step after equilibrium.
(2) If the failure criterion is satisfied, physically unload stresses to a lower level in the following time steps.
(3) Add phantom nodes after stress unloading is completed, and introduce overlapping elements.
(4) Update new residual force and stiffness for overlapping elements, assemble new global residual force and stiffness, and solve for the new geometry.

REPRESENTATIVE RESULTS

For the computational analyses, 40 parent Zircaloy-2 grains were oriented based on a loading plane of (0001) and a loading direction of $[2\bar{1}\bar{1}0]$. A convergent plane strain FE mesh of 6,466 elements was used for a mesh of 5mm ×8mm. Displacements were applied along the loading direction (Fig. 1). It was assumed that he maximum Euler angle misorientation is less than 15^0 for a random low angle misorientation distribution.

INTERGRANULAR AND TRANSGRANULAR FRACTURE

We investigated fracture behavior with hydride and twin distributions as shown in the Figure 1 for at quasi-static loading conditions at different temperatures.

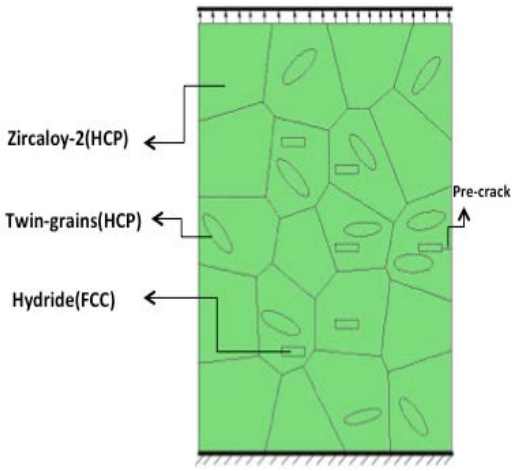

Fig. 1 Distribution of hydrides, twins, with a pre-crack

The ZrH2 hydrides have a f.c.c. structure, and we use orientation relations (ORs) to relate these hydrides to the h.c.p. matrix. As shown in Figure 3, a pre-crack cuts through the hydride in a brittle planar intergranular mode. The cracks are propagated along the basal cleavage planes. The effects of the ORs can also be clearly seen in the distribution of the normal stresses (Figures

2 a-b). At a nominal strain of 4%, the maximum normalized stress occurred ahead at the crack front with a maximum normalized value of approximately 4. For the case without ORs, the maximum value was 8 in the same region, which is twice the value of the ORs case.

(ɐ) (q)

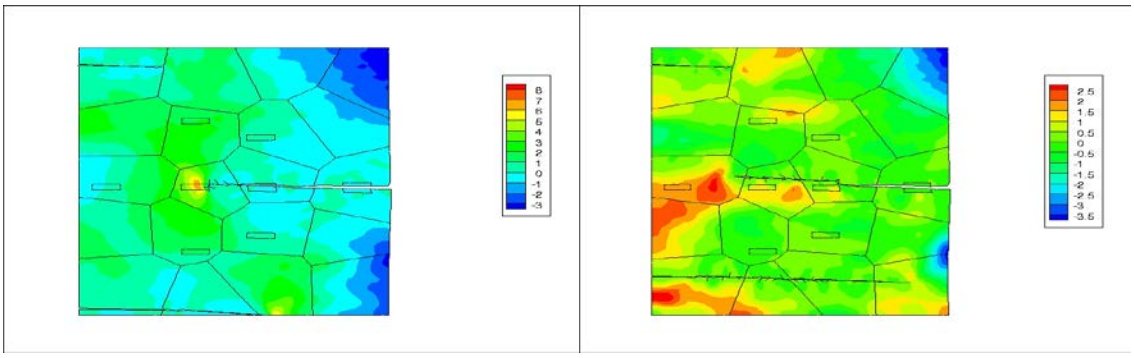

Fig. 2 Normal stress at (a) no ORs (b) with ORs at 4% nominal strain

ZrH hydrides have a b.c.c. structure, and they are semi-coherent with the h.c.p. zircaloy matrix. Hence, we need to account for both misfit strains and ORs. For the misfit strains, we modified our inelastic deformation-rate tensor by accounting for lattice misfit strains by incorporating the misfit strains, as normal deformation rates along the basal planes. The misfit strains are incorporated as initial strains and randomly distributed around the ZrH hydrides. The presence of misfit strains has a significant effect on crack paths and propagation. As seen in Figure 3, the crack path is affected by the presence of the misfit strains; these strains cause the crack to deviate and it also results in a higher fracture toughness.

(a) (b)

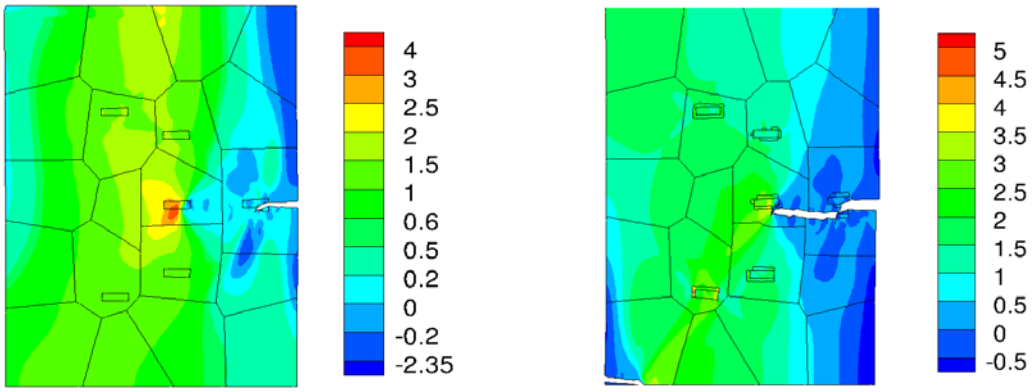

Fig. 3 Normal stress (a) with ORs (b) with ORs and misfit-strains at 3% nominal strain

We also investigated crack growth and propagation for an aggregate with hydrides and twins (Fig. 4). As seen below, the crack growth is transgranular and curved due to the twin

and hydride distributions and interfacial OR with the h.c.p. matrix. The cracks propagated along the basal cleavage planes, but the significant dislocation-density activity was along the

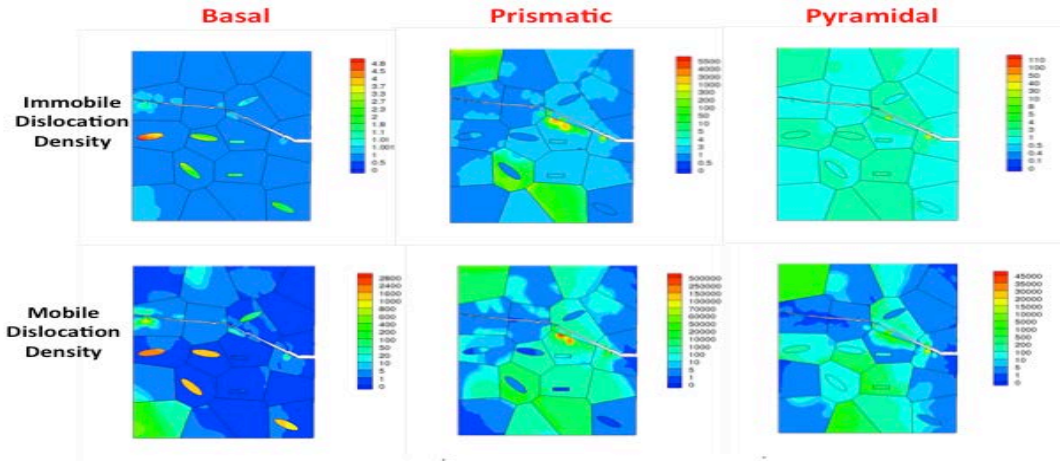

Fig. 4 Crack growth in a Zircaloy aggregate with twins, largest dislocation densities are along prismatic and pyramidal planes, dislocation activity affects crack paths

We are currently developing models for intergranular based on the diffusion of iodine products into the GBs of zircaloys. As indicated by Park et al. [11], iodine pits are randomly distributed along the grain surfaces in different shapes and sizes that range in size from 2.5 to 5.0 ums with average grain diameters of approximately 40 ums. When iodine is adsorbed into the zirconium cladding, the zirconium bond at the GB is weakened and the surface energy is consequently reduced. Free iodine gas can react with zirconium to form solid iodides and a gaseous zirconium tetra-iodide (ZrI4). The gaseous ZrI4 can then be decomposed easily into the iodine at a strained surface when hoop stress is applied; thus, pits are formed due to a localized attack on the GB. Due to this, the GB is embrittled because it has a large amount of impurities such as Fe, Al, Si and Cr, and if sufficient external stress is applied to the surface, then a slip band forms around a GB surface, thereby increasing instability. We have accounted for these pits through modifying our Voronoi tessellation scheme that is used to generate our finite-element mesh that is physically representative of pit morphology, grain and GB morphologies. As these results indicate, shear strain accumulated at the pit interfaces (Fig. 5), which delineates how these interfaces are the nucleation sites for intergranular fracture.

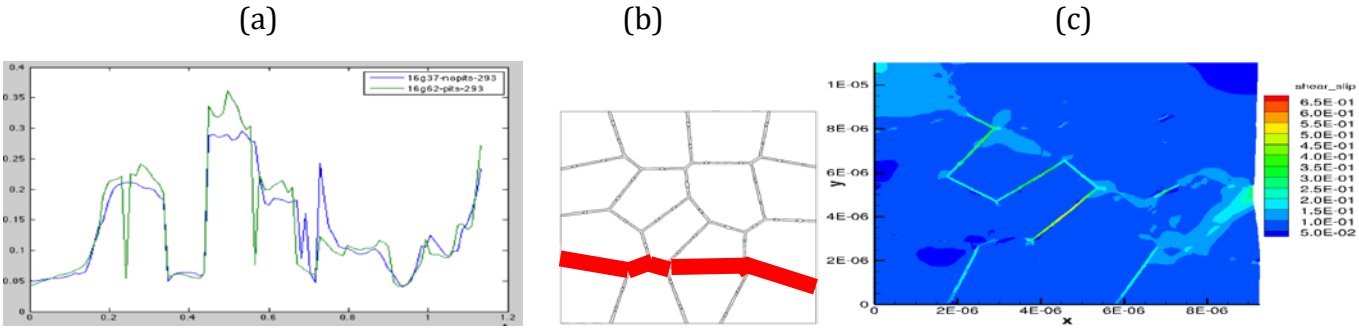

Fig. 5 (a) GB locations of accumulations along GB indicated in (b), (c) Strain accumulation at the pits, which are preferential sites for GB at 5% nominal strain of

SUMMARY and FUTURE RESEARCH OBJECTIVES

We have presented a dislocation density based multiple slip crystal plasticity formulation, which is coupled to a nonlinear fracture methodology, that accounts for ORs between f.c.c. (ZrH2) and b.c.c. (ZrH) precipitates and an h.c.p. zircaloy matrix. We investigated the effects of ORs for an aggregate with and without cracks subjected to different loading conditions. We obtained unique ORs between parallel directions and planes between the relevant f.c.c. and h.c.p. systems. The ORs and misfit strains significantly affected local behavior, in aggregates without cracks, such as shear slip accumulation, dislocation-density evolution, lattice rotation, and thermal and stress buildup. These local mechanism can be used for predictions of transgranular and intergranular fracture. We have also investigated why twins increase strength and fracture toughness. We have also incorporated iodine pits within Voronoi physically realistic structures. Future objectives will be focused on

(i) Investigating how pit formation leads to intergranular fracture at room and high temperatures;

(ii) Modeling the how the presence of ZrH and ZRH2 within the same aggregate affect fracture and trying to assess how hydrides reorient as a function of temperature;

(iii) Understanding how temperature affects trangranular and intergranular fracture through a portioning of diffusive conductive and dissipative adiabatic heating mechanisms.

REFERENCES

[1] L. Capolungo, I. J. Beyerlein, G. C. Kaschner, and C. N. Tomé: *Materials Science and Engineering: A*, 2009, vol. 513–514, pp. 42.

[2] S. Mendelson: *J. Appl. Phys.*, 1970, vol. 41, pp. 1893.

[2] M. H. Yoo, J. R. Morris, K, S. R. Agnew, and K. M. Ho: *Metall. Mat. Trans. A*, 2002, vol. 33A, pp. - 813-822.

[3] C. Mareau and M. R. Daymond: *Materials Science and Engineering: A*, 2011, vol. 528, pp. 8676.

[4] Cheadle B. A. and Ells C. E.: - *Journal of Nuclear Materials*, , pp. - 240.

[5] M. H. Yoo: *Metall. Trans. A*, 1981, vol. 12A, pp. - 409-418.

[6] M. H. Yoo, S. R. Agnew, J. R. Morris, and K. M. Ho: *Materials Science and Engineering: A*, 2001, vol. 319–321, pp. 87.

[7] L. Capolungo: *Acta Materialia*, 2011, vol. 59, pp. 2909.

[8] Lin Xiao and Haicheng Gu: *Metall. Mat. Trans. A*, 1997, vol. 28A, pp. - 1021-1033.

[9] P. Shanthraj and M. A. Zikry: *Acta Materialia,* 2011, vol. 59, pp. 7695.

[10] M. A. Zikry: *Comput. Struct.,* 1994, vol. 50, pp. 337.

[11] S.Y. Park, J.H. Kim, B.K. Choi, Y.H. Jeong, *Met. Mater. Int.*, 2007 13 (2) 155.